Catalysis Today 149 (2010) 248–253

Contents lists available at ScienceDirect

Catalysis Today

journal homepage: www.elsevier.com/locate/cattod

Ruthenium supported on new TiO_2–ZrO_2 systems as catalysts for the partial oxidation of methane

Valerio Choque, Pilar Ramírez de la Piscina, Daniel Molyneux, Narcís Homs *

Department of Inorganic Chemistry and Institute of Nanoscience and Nanotechnology, Universitat de Barcelona, C/Martí i Franquès 1-11, 08028 Barcelona, Spain

ARTICLE INFO

Article history:
Available online 1 November 2009

Keywords:
Partial oxidation of methane
TiO_2–ZrO_2 supports
Supported Ru catalysts
Syngas

ABSTRACT

The partial oxidation of methane is studied at 673–873 K over new Ru-based catalysts supported on TiO_2–ZrO_2 with different TiO_2 content. Supports were prepared by a sol–gel method, and $RuCl_3$ and $RuNO(NO_3)_3$ were used as ruthenium precursors to prepare the catalysts (1–2 wt% Ru). The effect of the reaction temperature on the catalytic behavior is analyzed, along with the support composition and the Ru precursor used.

1. Introduction

Ru-based catalysts have been shown to be effective in the catalytic partial oxidation of methane (CPOM):

$$CH_4 + (1/2)O_2 \rightarrow CO + 2H_2 \qquad \Delta H_{298} = -35.7\ \text{kJ/mol}$$

This process can provide synthesis gas in an H_2/CO of 2:1 which can be used directly as feedstock for the methanol or Fischer–Tropsch synthesis. CPOM is a more favorable and efficient process, from the energetic point of view, than the highly endothermic methane steam reforming reaction [1–11]. Other proposed applications of CPOM are the partial conversion of methane into a H_2-enriched stream for the enhancement of gas turbine performances and the production of suitable synthesis gas for fuelling solid oxide fuel cells [7].

The exothermicity and fastness of the process allow the use of compact reformers with reduced thermal inertia and the achievement of both high methane conversion and high selectivity to H_2 operating at short contact time (ca. 10^{-3} s) [6,7]. However, for using the CPOM in an industrial scale several problems must still to be solved. Regarding the catalysts, they can irreversibly be damaged by local hot-spots due to the exothermic methane combustion; after the methane combustion, reforming processes of CH_4 with CO_2 and H_2O could take place. On the other hand, direct formation of CO and H_2 has been proposed for avoiding high hot-spot temperatures [3]. Noble metals show a high activity in the CPOM and a high resistance against coke formation. Over noble metals both the indirect mechanism *via* the total oxidation of methane and the direct mechanism of formation of CO and H_2 have been proved to exist. The direct formation of CO and H_2 requires the presence of reduced metal surface sites where the decomposition of methane can occur [12,13].

The stabilization of the Ru^0 active phase under reaction conditions has been shown to greatly influence the behavior of Ru-based catalysts in the CPOM [4,12,13]. The support plays a main role in this stabilization. In this context, the stabilization of Ru^0 in Ru/TiO_2 under CPOM conditions at 973–1073 K has been claimed to be the agent responsible for the high selectivity to synthesis gas shown by Ru/TiO_2 catalysts [4].

We have previously reported the behavior of ruthenium supported catalysts on mixed oxides Ta_2O_5–ZrO_2 and Nb_2O_5–ZrO_2 in the CPOM at 673–873 K; a better behavior in the CPOM of the catalysts supported on mixed systems was demonstrated when the behavior of these catalysts was compared to that of catalysts supported on pure Ta_2O_5, Nb_2O_5 or ZrO_2 oxides [14]. Here, we report a study of new Ru-based catalysts supported on mixed systems TiO_2–ZrO_2 prepared by a sol–gel method. The effect of both the support composition and the precursor of ruthenium used is also reported.

2. Experimental

For the preparation of TiO_2, ZrO_2 and TiO_2–ZrO_2 materials, a sol–gel method was used using titanium ethoxide and zirconium propoxide in a similar manner as reported previously for other mixed systems [15]. Propanol solutions of titanium and/or zirconium precursors were prepared under Ar and mixed at room temperature over an aqueous solution of propanol. Suspensions were maintained at 343 K for 6 h with stirring and then at 298 K for 16 h. Solids were filtered, dried at 383 K and calcined at 873 K. Solids were labeled *x*TiZr where *x* accounts for the wt/wt (%) of TiO_2 in the support. Aqueous solutions of $Ru(NO)(NO_3)_3$ or $RuCl_3$ were

* Corresponding author. Tel.: +34 934037056; fax: +34 934907725.
E-mail address: narcis.homs@qi.ub.es (N. Homs).

0920-5861/$ – see front matter © 2009 Elsevier B.V. All rights reserved.
doi:10.1016/j.cattod.2009.09.017

used to impregnate the supports by the incipient wetness method to obtain ca. 1–2% (wt/wt) of Ru. Samples were dried at 373 K, then calcined at 573 K and labeled Ru(NO)/support or Ru(Cl)/support depending on the Ru precursor used.

The chemical composition of the supports was determined by X-ray fluorescence analysis using a Phillips PW-2400 apparatus and the Ru content of catalysts was analyzed by Inductively Coupled Plasma (ICP) in a PerkinElmer 3200RL Optima spectrometer.

The BET surface area of the samples was determined by nitrogen adsorption at 77 K using a Micromeritics ASAP9000 instrument.

A Micromeritics AutoChem II Chemisorption Analyzer was used for the Temperature Programmed Reduction (TPR) and CO chemisorption experiments. Calcined samples were heated (10 K/min) with a 12.5% H_2/Ar mixture (50 mL/min) up to 623 K and the hydrogen consumption was measured by a thermal conductivity detector. CO chemisorption was determined at 308 K. Two different series of CO chemisorption experiments were carried out; one of them after the TPR experiment and the other one after the catalytic test at 773 K.

The supports, and the catalysts after calcination, reduction and post-reaction were analyzed by X-ray powder diffraction (XRD). XRD patterns were obtained using a Bragg–Brentano PANalytical X'Pert PRO MPD Alpha1 X-ray diffractometer with nickel-filtered Cu Kα1 radiation (λ = 0.15406 nm). The XRD profiles were collected in the 2θ angle between 20° and 100°, at the step width of 0.017° and by counting 50 s at each step. The XRD patterns of samples were compared to the corresponding JCPDS files.

The X-ray photoelectron spectra (XPS) of fresh (calcined) and used catalysts were obtained using a Sage HR (Specs GmbH) spectrometer equipped with an Al Kα X-ray exciting source calibrated using the Ag $3d_{5/2}$ line. The residual pressure in the analysis chamber was maintained below 10^{-8} Torr. The binding energies (BEs) were referred to the C1s peak at 284.9 eV which gave BE values with an accuracy of ±0.1 eV. The Ru 3d, Ti 2p, Zr 3d and Cl 2p atomic levels were analyzed. Residual chlorine was not detected in the studied samples.

CO chemisorption was followed by infrared spectroscopy (FTIR) using a Nicolet 5700 Nexus Fourier transform spectrometer. The spectra were obtained at room temperature at a resolution of 4 cm^{-1} by collecting 128 scans. Special greaseless cells with CaF_2 windows, which allowed vacuum and thermal treatments were used. Samples were reduced in the cell with repeated treatments with H_2 at 623 K followed by a high vacuum treatment at the same temperature. Reduced or post-reaction samples were contacted with CO (27 kPa) and the corresponding spectrum was taken after a vacuum treatment at 373 K.

Catalytic tests were performed in a stainless steel continuous fixed-bed microreactor with on-line GC analysis of products; SiC was used to dilute the catalysts. The reaction conditions were P_T = 4 bar, T = 673–873 K, GHSV = 6500 h^{-1}, $CH_4/O_2/He$ = 6/1/22 molar ratio. The selectivity of the products obtained: CO, CO_2 and H_2, was calculated as the molar ratio of each product with respect to the total amount of products obtained (% mol/mol). In a standard catalytic test the temperature of the catalyst (calcined sample) was raised under He flow up to 573 K; then, the reactant mixture was introduced and temperature increased up to 673 K. The catalysts were kept at this temperature for 4 h and then the temperature was subsequently increased up to 773 K and maintained for 4 h (standard catalytic tests) or 24 h (long time catalytic tests). The methane conversion was in the range 12–24%. The Ru(Cl)/4TiZr was tested at 873 K and with CO_2 co-feeding (2.5 and 5%, v/v).

3. Results and discussion

Table 1 shows the BET surface area of *x*TiZr samples prepared with different Ti content. The BET surface area increased with the Ti content till 34TiZr and then progressively decreased. Fig. 1 depicts the XRD patterns corresponding to the supports after calcination at 873 K. As expected, pure ZrO_2 shows diffraction peaks corresponding to tetragonal and monoclinic ZrO_2. Although the XRD patterns of *x*TiZr supports ($x \leq 18$) and 44TiZr also indicated the presence of crystalline monoclinic and tetragonal ZrO_2, a displacement of the position of the diffraction peaks with respect to those of pure ZrO_2 can be noted. Inset in Fig. 1 shows the (0 1 1) most intense peak of ZrO_2 tetragonal phase, the maximum of this peak is displaced to higher 2θ values when the titanium content increases in the support according to the presence of Ti(IV) in the crystalline tetragonal ZrO_2. In contrast, XRD pattern of 34TiZr does not show diffraction peaks indicating the formation of an amorphous material. Diffraction peaks corresponding to anatase TiO_2 phase are distinguished from the diffraction pattern of 65TiZr and pure TiO_2. Peaks corresponding to anatase are located at lower 2θ in the diffraction pattern of 65TiZr; this may be related with the presence of Zr(IV) in the crystalline TiO_2. XRD patterns of calcined catalysts are similar to those of the corresponding supports. Only in the case of Ru(NO)/34TiZr was it possible to distinguish a peak at 2θ = 54.2° assigned to the most intense (2 1 1) reflection of the crystalline RuO_2 phase, the particle size determined by the Scherrer equation was 15 nm. In the XRD pattern of Ru(Cl)/34TiZr we found no peaks that indicated a small size of crystalline particles of RuO_2 if these were present in this catalyst. In all the other catalysts, the presence of crystalline RuO_2 could not be determined because the peaks of support would mask those of RuO_2.

Table 1
TiO_2 content and BET surface area of supports.

Support	TiO_2 (%, wt/wt)	BET (m^2/g)
ZrO_2	–	33
4TiZr	4.4	37
10TiZr	9.7	36
18TiZr	18.2	50
34TiZr	34.3	147
44TiZr	44.2	70
65TiZr	65.1	47
TiO_2	–	20

Fig. 2 depicts the TPR profile of catalysts. Hydrogen consumption peaks between 375 and 460 K were found which were

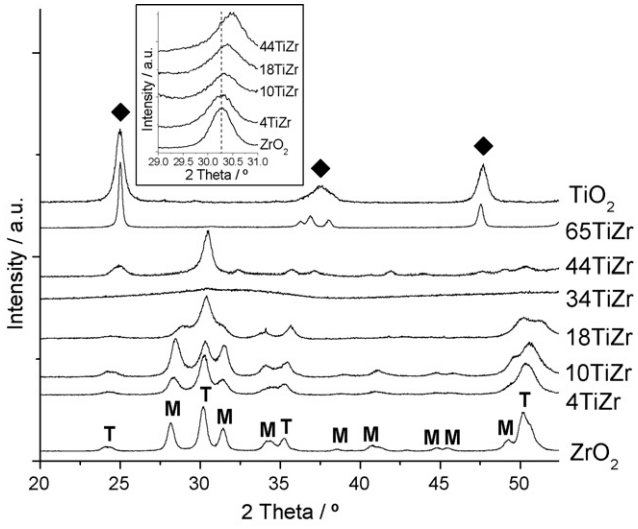

Fig. 1. XRD patterns of supports after calcination at 873 K. (M) Diffraction peaks characteristic of monoclinic ZrO_2; (T) diffraction peaks characteristic of tetragonal ZrO_2; (◆) diffraction peaks characteristic of anatase TiO_2. Inset: location of the (0 1 1) most intense XRD peak of the tetragonal ZrO_2 phase.

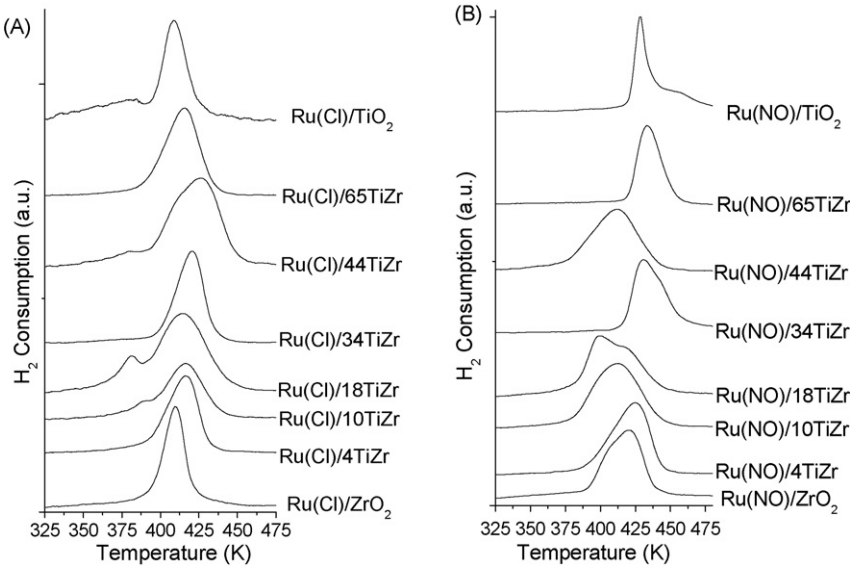

Fig. 2. H_2-TPR diagram of catalysts: (A) Ru(Cl)/*x*TiZr and (B) Ru(NO)/*x*TiZr.

assigned to the reduction of well-dispersed RuO_x and RuO_2 particles, at lower and higher temperatures respectively. The majority of catalysts showed a H_2 consumption of ca. 2 mol H_2/mol Ru which corresponds to the stoichiometric reduction of RuO_2 to Ru (see Table 2). However, the low amount of H_2 consumed (ca. 1 mol H_2/mol Ru) in the case of the Ru(Cl)/TiO_2 catalyst, may be related with the presence in this catalyst of oxidized ruthenium species strongly interacting with the support, which could not be reduced at the maximum temperature used in the TPR experiment (623 K). The presence of reduction peaks at high temperature has been shown for Ru/Al_2O_3 and Ru/MgO–Al_2O_3 catalysts with low Ru loadings (1%, wt/wt) [16,17]. After the TPR experiments carried out up to 623 K, the mean particle size was determined by CO chemisorption at 308 K. The corresponding mean particle size was calculated assuming a stoichiometry CO:Ru 1:1 and a spherical shape of Ru particles (results are shown in Table 2). The smaller particle sizes (8–12 nm) were found for Ru(Cl)/*x*TiZr ($4 \leq x \leq 18$) samples and for these catalysts the Ru particle size increases with the Ti content. Higher particle sizes were found for the Ru(Cl)/*x*TiZr samples with higher Ti content ($34 \leq x \leq 65$), which showed sizes in the range (26–35 nm). A previous work of ours had compared the use of $Ru(NO)(NO_3)_3$ and $RuCl_3$ as ruthenium precursors in the preparation of catalysts supported on Ta_2O_5–ZrO_2 and Nb_2O_5–ZrO_2 materials; in general lower particle sizes were obtained when $RuCl_3$ was used as ruthenium precursor than when $Ru(NO)(NO_3)_3$ was used, and the Ru particle size increased with the increase of the content of Ta_2O_5 or Nb_2O_5 [14]. In this work, for Ru/*x*TiZr catalysts with low TiO_2 contents ($4 \leq x \leq 18$) a similar trend was found, and the particle size corresponding to the catalysts prepared from $RuCl_3$ was lower than that of catalysts prepared from $Ru(NO)(NO_3)_3$ with an increase in the Ru particle size being noted in both cases when the Ti content increases. The particle size of Ru after the TPR experiment was also determined from the XRD pattern using the Scherrer equation (see Table 2). Ru/*x*TiZr catalysts with high Ti content ($34 \leq x \leq 65$) showed values of particle size determined by CO chemisorption significantly higher than those determined from XRD patterns; this may be related with a partial coverage of the surface ruthenium particles with TiO_x.

Calcined catalysts at 573 K were tested in the CPOM reaction at 673 K, then at 773 K; later, they were characterized by XRD, CO chemisorption, FTIR with CO as probe molecule and XPS. XRD

Table 2
Ruthenium content (%, wt/wt) and other characteristics of the catalysts.

Sample	%Ru	mol H_2/mol Ru (TPR)[a]	d Ru[b] DRX (nm)	d Ru[b] (CO) (nm)	d Ru[c] XRD (nm)	d Ru[c] (CO) (nm)
Ru(NO)/ZrO_2	2.3	2.1	17	15	13	18
Ru(NO)/4TiZr	2.0	2.4	12	18	15	22
Ru(NO)/10TiZr	1.8	2.3	14	20	14	13
Ru(NO)/18TiZr	1.8	1.9	19	21	13	18
Ru(NO)/34TiZr	1.9	2.0	15	26	15	22
Ru(NO)/44TiZr	1.9	2.3	13	17	16	22
Ru(NO)/65TiZr	1.8	2.3	15	24	13	27
Ru(NO)/TiO_2	2.0	1.8	28	29	24	28
Ru(Cl)/ZrO_2	1.4	1.8	15	11	12	15
Ru(Cl)/4TiZr	1.4	2.0	10	8	8	14
Ru(Cl)/10TiZr	1.5	1.8	9	10	14	17
Ru(Cl)/18TiZr	1.3	2.0	9	12	11	20
Ru(Cl)/34TiZr	1.2	2.1	24	35	10	14
Ru(Cl)/44TiZr	1.4	1.7	12	27	11	17
Ru(Cl)/65TiZr	1.3	2.4	14	26	11	18
Ru(Cl)/TiO_2	1.4	1.0	21	24	n.d.	24

[a] Hydrogen consumption in the TPR experiment.
[b] Mean crystallite size of Ru particles determined from DRX or CO chemisorption after the TPR experiments.
[c] Mean crystallite size of Ru particles determined from DRX or CO chemisorption after the catalytic test at 773 K.

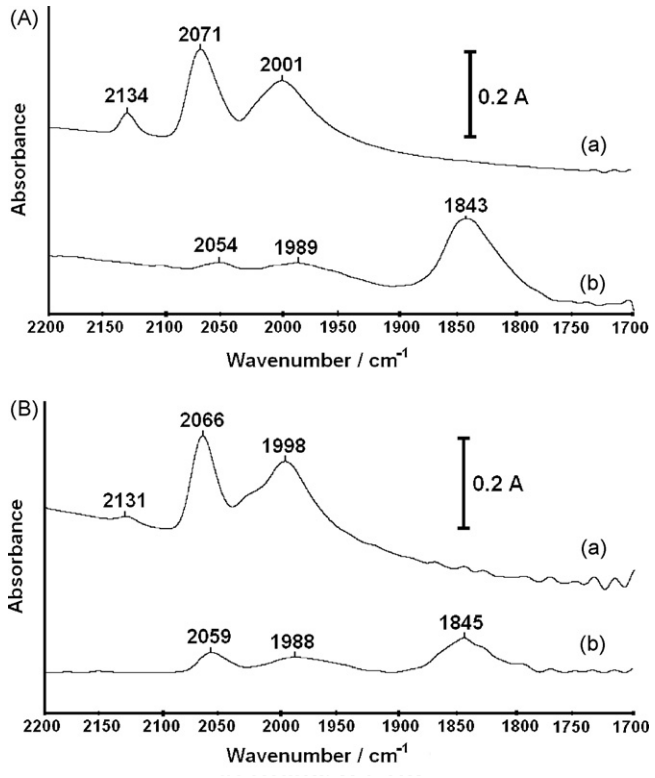

Fig. 3. FTIR spectra in the υ(CO) region of CO adsorbed on: (A) Ru(Cl)/4TiZr and (B) Ru(NO)/4TiZr. Spectra (a) correspond to the CO adsorption on reduced catalysts. Spectra (b) correspond to the CO adsorption on post-reaction catalysts after the CPOM at 773 K.

patterns of post-reaction catalysts showed in all cases the corresponding diffraction peaks of the support and a peak at $2\theta = 44.0^{\circ}$. This peak corresponds to the most intense (1 0 1) reflection of the Ru_{hcp} phase.

As stated above, a peak at $2\theta = 54.2^{\circ}$ was visible in the XRD pattern of calcined Ru(NO)/34TiZr catalyst; the absence of this peak in the XRD pattern of post-reaction catalyst accords with the reduction of RuO_2 under reaction conditions. Using the Scherrer equation, the mean size of Ru^0 particles obtained after CPOM was determined; values in the range 13–16 nm were obtained for Ru(NO)/TiZr and in the range 8–14 nm for Ru(Cl)/TiZr (Table 2). Table 2 also shows the mean particle size determined by CO chemisorption; in general, higher values were obtained when they are compared to those obtained from XRD patterns, and this may be interpreted in terms of the formation of aggregates of Ru crystallites or by the partial decoration of the Ru particles with species coming from the support.

Catalysts Ru(Cl)/4TiZr and Ru(NO)/4TiZr were analyzed by XPS both before and after the catalytic test. Calcined catalysts before the catalytic test showed a BE corresponding to the Ru $3d_{5/2}$ level of 280.7–280.8 eV and this is characteristic of RuO_2. After the CPOM the BE corresponding to the Ru $3d_{5/2}$ was 279.7–279.8 eV, according to the presence of Ru^0.

Under CPOM conditions, the reduction of the initial RuO_2 phase and the formation of metallic ruthenium can be proposed, probably due to the reaction:

$$CH_4 + 2RuO_2 \rightarrow CO_2 + 2Ru + 2H_2O$$

which has been proposed to occur in supported Ru catalysts under CPOM reaction conditions [18].

After the CPOM at 773 K, Ru(Cl)/4TiZr and Ru(NO)/4TiZr samples were also analyzed by FTIR using CO as probe molecule. Spectra of CO chemisorbed on post-reaction catalysts are compared to those obtained after the CO chemisorption on reduced catalysts. Fig. 3A and B shows this comparison for Ru(Cl)/4TiZr and Ru(NO)/4TiZr, respectively. When CO was chemisorbed on reduced catalysts three main bands with maxima at 2130–2135 cm^{-1}, 2065–2075 cm^{-1}, and 1995–2005 cm^{-1} appeared (spectra a in Fig. 3A and B). The band with maximum at 2130–2135 cm^{-1} and the high wavenumber part of the broad band centred at 2065–2075 cm^{-1} are assigned to multicarbonyl species on Ru^{2+} cations [19]. These species can be produced by corrosive chemisorption of CO on small particles of Ru or by direct adsorption of CO over partially reduced samples [20]. The part of the band with a maximum at 2065–2075 cm^{-1} located at low wavenumbers is attributed to CO linearly adsorbed on Ru sites. On the other hand, the broad bands with maxima at ca. 2000 cm^{-1} could be due to CO adsorbed on isolated Ru^0 entities of very low nuclearity. As regards the FTIR patterns obtained after the CO chemisorption on post-reaction catalysts (spectra b in Fig. 3A and B), a main band with maximum at ca. 1845 cm^{-1} appeared. The low wavenumber of this band could be due to the presence of electron-donor species in the vicinity of the adsorption sites; it is probable that surface carbon species formed under reaction conditions. However, the presence of new bridged CO species, C-bonded and O-bonded to Ru^0 and oxidized centres of the support, respectively, cannot be ruled out. Besides the band at ca. 1845 cm^{-1}, low intensity bands located at ca. 2055 cm^{-1} and 1988 cm^{-1} raised after the CO adsorption on post-reaction samples; these bands can be related to linear CO on well-dispersed Ru particles [21] according to a low sintering of ruthenium particles during the reaction. On the other hand, no bands corresponding to CO adsorbed on oxidized Ru were detected when CO was contacted with the post-reaction samples.

The catalytic behavior of calcined samples in the CPOM depended on the temperature, TiO_2 content of the support and the Ru precursor used in the preparation of catalysts. High selectivity to CO_2 was obtained in all cases at 673 K according to former results over Ru/Ta_2O_5–ZrO_2 or Ru/Nb_2O_5–ZrO_2 systems [14]. This high selectivity to CO_2 is related with the methane total oxidation which is a reaction likely catalyzed by the RuO_2 initially present in the catalysts.

$$CH_4 + 2O_2 \rightarrow CO_2 + 2H_2O$$

At 773 K, catalysts were active in the partial oxidation of CH_4, and H_2, CO and CO_2 were obtained as products probably as consequence of the transformation under reaction conditions of RuO_2 to Ru, as was determined by XRD, XPS and FTIR of CO chemisorption. Several studies on CPOM over Ru catalysts points to the dependence of reaction mechanism on the reaction temperature and the mechanism has been related with the oxidation state of Ru. The direct formation of CO and H_2 requires the presence of reduced metal surface sites where the decomposition of methane can occur. The combustion-reforming mechanism requires oxidized metal sites as well as reduced sites; the methane combustion may take place on the oxidized sites and then metallic sites could catalyze reforming reactions [4,13,18].

Ru/*x*TiZr catalysts were more active and selective to syngas than Ru/TiO_2 catalysts (Table 3). Over Ru/TiO_2, high selectivity to CO_2 and low selectivity to H_2 were obtained; over this catalyst the total oxidation of CH_4 would be more favored than over Ru/*x*TiZr systems. On the other hand, the catalytic activity of catalysts per mol of Ru was higher for Ru(Cl)/TiZr in comparison with those of Ru(NO)/TiZr; this can be related with the smaller particle size of Ru^0 observed after reaction for the catalysts prepared using $RuCl_3$ as precursor (see Table 2). Turnover frequency number (TOF) referred to methane transformed was calculated from the CO chemisorption experiments carried out on the post-reaction

Table 3
Catalytic behavior of catalysts in the partial oxidation of methane after 4 h of reaction at 773 K.

Catalyst	CH_4 conv. (%)	Activity mol CH_4/mol Ru × h	TOF[a] (s^{-1})	Selectivity (%, mol/mol)			H_2/CO (mol/mol)
				H_2	CO	CO_2	
Ru(NO)/ZrO_2	19	273	1.0	56.0	21.4	22.6	2.6
Ru(NO)/4TiZr	22	364	1.7	53.5	20.0	26.4	2.7
Ru(NO)/10TiZr	23	419	1.2	53.3	23.2	23.5	2.3
Ru(NO)/18TiZr	24	443	1.7	53.3	26.0	20.7	2.1
Ru(NO)/34TiZr	20	360	1.7	50.1	22.1	27.8	2.3
Ru(NO)/44TiZr	18	326	1.5	52.5	21.2	26.3	2.4
Ru(NO)/65TiZr	20	366	2.0	51.6	20.0	28.4	2.6
Ru(NO)/TiO_2	13	220	1.3	35.4	8.3	56.3	4.3
Ru(Cl)/ZrO_2	22	472	1.5	53.7	19.9	26.4	2.7
Ru(Cl)/4TiZr	22	548	1.6	52.1	20.8	27.1	2.5
Ru(Cl)/10TiZr	22	470	1.5	50.6	23.7	25.6	2.1
Ru(Cl)/18TiZr	20	525	2.2	51.4	20.8	27.8	2.5
Ru(Cl)/34TiZr	19	517	1.4	52.4	21.0	26.6	2.5
Ru(Cl)/44TiZr	19	459	1.6	52.7	20.2	27.1	2.6
Ru(Cl)/65TiZr	22	556	2.1	53.4	19.8	26.8	2.7
Ru(Cl)/TiO_2	12	276	1.4	28.0	5.4	66.6	5.2

[a] Calculated from CO chemisorption results on post-reaction catalysts.

samples. Samples Ru/*x*TiZr showed TOF values in the range 1.2–2.2 s^{-1} (Table 3).

Long-term catalytic tests at 773 K were carried out over several Ru/*x*TiZr catalysts; samples showed a very stable catalytic behavior throughout the reaction time (24 h). Fig. 4 shows the methane conversion values and the product distribution corresponding to Ru(Cl)/18TiZr (Fig. 4A) and Ru(NO)/18TiZr (Fig. 4B).

We also studied the CPOM at 873 K over Ru(Cl)/4TiZr and the influence of the CO_2 co-feeding. In the absence of CO_2, an increase

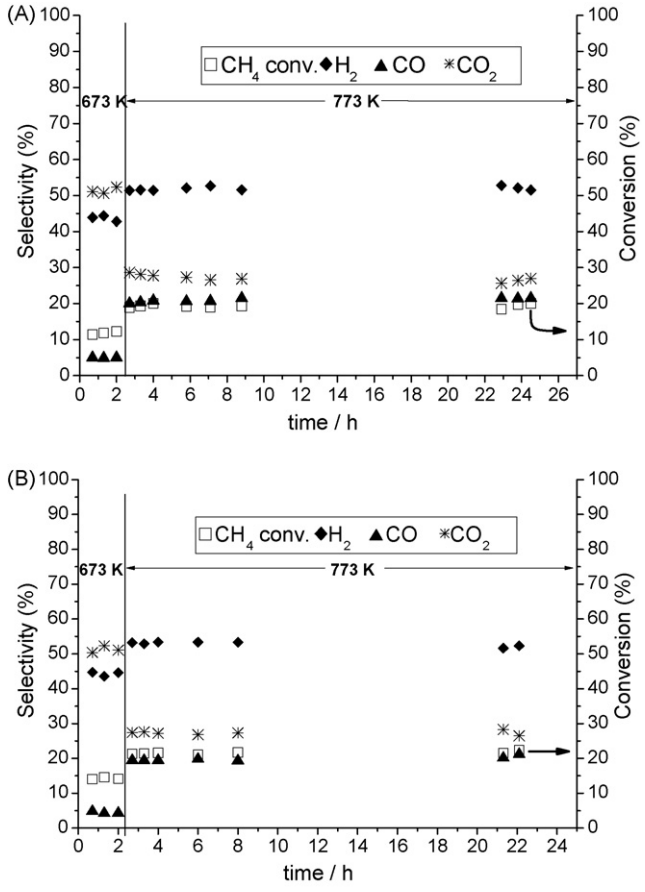

Fig. 4. Catalytic behavior in the CPOM of several catalysts at 773 K. (A) Ru(Cl)/18TiZr and (B) Ru(NO)/18TiZr. Reaction conditions: P_T = 4 bar, GHSV = 6500 h^{-1}, CH_4/O_2/He = 6/1/22.

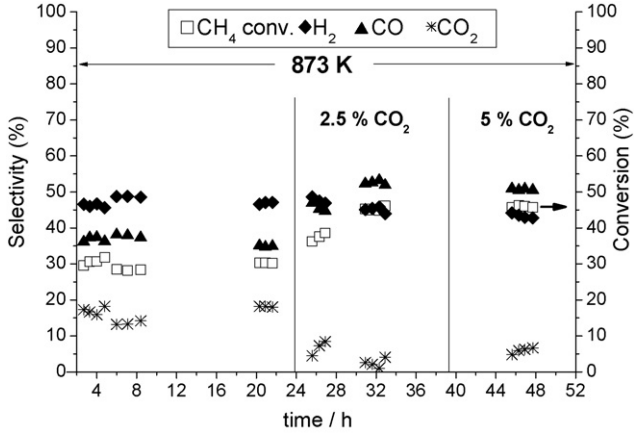

Fig. 5. Catalytic behavior in the CPOM of Ru(Cl)/4TiZr at 873 K. Reaction conditions: P_T = 4 bar, GHSV = 6500 h^{-1} and CH_4/O_2/He = 6/1/22. After 24 h of reaction, CO_2 was co-fed in the reactants, 2.5% (v/v) CO_2 and then 5% (v/v) CO_2.

of temperature from 773 K to 873 K produced an increase in the CH_4 conversion and CO selectivity, while a decrease of CO_2 selectivity was noted (see in Table 3 and left-part in the graph of the Fig. 5). These changes in the selectivity produced a decrease in the H_2/CO ratio (The H_2/CO ratio was ca. 2.5 at 773 K and 1.3 at 873 K). In these conditions the catalytic behavior was stable at least for 20 h (see Fig. 5). Metallic ruthenium was probably stabilized under these conditions and the methane combustion was minimized. Fig. 5 also shows that the co-feeding of CO_2 produces an increase in the methane conversion and the CO selectivity, and a decrease in the CO_2 selectivity. Under these conditions, the H_2/CO ratio was ca. 1 and a TOF of 4.1–5.1 s^{-1} was estimated from data of CO chemisorption on this post-reaction sample. The CO generation from CO_2 may take place through the dry reforming and/or the reverse of water gas shift reaction. Moreover, the CO_2 presence could favor a constant removal of carbonaceous or CH*x* surface species from the surface, generating CO and H_2.

4. Conclusions

New TiO_2–ZrO_2 supports prepared by a sol–gel method were appropriate for the preparation of supported ruthenium catalysts used in the CPOM. The initial presence of the RuO_2 phase is related with the total oxidation of methane. Ru^0 formed under reaction

conditions at 773 K, and this was determined from XRD, XPS and FTIR with CO as probe molecule experiments.

Catalysts Ru/*x*TiZr were more active and showed lower selectivity to CO_2 than those supported on pure TiO_2. The use of $RuCl_3$ as precursor in the preparation of catalysts led to higher values of activity per mol of Ru than the use of $Ru(NO)NO_3$ precursor, this probably being a consequence of the lower particle size of Ru in the former catalysts.

Acknowledgements

The authors are grateful to the Spanish and Catalan governments for financial support (research projects MAT2008-02561 and 2009SGR-0674, respectively). V. Choque acknowledges an AECI-MAE grant and D. Molyneux the Erasmus exchange program between the University of Barcelona and the University of Aberdeen.

References

[1] A.T. Ashcroft, A.K. Cheetham, J.S. Foord, M.L.H. Green, C.P. Grey, A.J. Murrell, P.D.F. Vernon, Nature 344 (1990) 319.
[2] M.A. Peña, J.P. Gomez, J.L.G. Fierro, Appl. Catal. A: Gen. 144 (1996) 7.
[3] D. Wolf, M. Höhenberger, M. Baerns, Ind. Eng. Chem. Res. 36 (1997) 3345.
[4] C. Elmasides, D.I. Kondarides, S.G. Neophytides, X.E. Verykios, J. Catal. 198 (2001) 195.
[5] A.P.E. York, T. Xiao, M.L.H. Green, Top. Catal. 22 (2003) 345.
[6] Q.G. Yan, T.H. Wu, W.Z. Weng, H. Toghiani, R.K. Toghiani, H.L. Wan, C.U. Pittman Jr., J. Catal. 226 (2004) 247.
[7] T. Bruno, A. Beretta, G. Groppi, M. Roderi, P. Forzatti, Catal. Today 99 (2005) 89.
[8] J. Requies, M.A. Cabrero, V.L. Barrio, J.F. Cambra, M.B. Güemez, P.L. Arias, V. La Parola, M.A. Peña, J.L.G. Fierro, Catal. Today 116 (2006) 304.
[9] A.C.W. Koh, L. Chen, W.K. Leong, B.F.G. Johnson, T. Khimyak, J. Lin, Int. J. Hydrogen Energy 32 (2007) 725.
[10] R. Lanza, S.G. Järas, P. Canu, Appl. Catal. A: Gen. 325 (2007) 57.
[11] R.M. Navarro, M.A. Peña, J.L.G. Fierro, Chem. Rev. 107 (2007) 3952.
[12] C. Elmasides, D.I. Kondarides, W. Grünert, X.E. Verykios, J. Phys. Chem. B 103 (1999) 5227.
[13] S. Rabe, M. Nachtegaal, F. Vogel, Phys. Chem. Chem. Phys. 9 (2007) 1461.
[14] V. Choque, N. Homs, R. Cicha-Szot, P. Ramírez de la Piscina, Catal. Today 142 (2009) 308.
[15] B. Samaranch, P. Ramirez de la Piscina, G. Clet, M. Houalla, P. Gélin, N. Homs, Chem. Mater. 19 (2007) 1445.
[16] P.S.S. Reddy, N. Pasha, M.G.V. Chalapathi Rao, N. Lingaiah, I. Suryanarayana, P.S. Sai Prasad, Catal. Commun. 8 (2007) 1406.
[17] L. Santos Carvalho, A. Rosa Martins, P. Reyes, M. Oportus, A. Albornoz, V. Vicentini, M.C. Rangel, Catal. Today 142 (2009) 52.
[18] S. Rabe, T.-B. Truong, F. Vogel, Appl. Catal. A: Gen. 292 (2005) 177.
[19] G.H. Yokomizo, C. Louis, A.T. Bell, J. Catal. 120 (1989) 1.
[20] K. Hadjiivanov, J.-C. Lavalley, J. Lamotte, F. Maugé, J. Saint-Just, M. Che, J. Catal. 176 (1998) 415.
[21] C. Elmasides, X.E. Verykios, J. Catal. 203 (2001) 477.